https://dx.doi.org/10.21577/0103-5053.20220067

J. Braz. Chem. Soc., Vol. 33, No. 9, 1017-1027, 2022

Communication

Anti-Hyperglycemic Activities, Molecular Docking and Structure-Activity Relationships (SARs) Studies of Endiandric Acids and Kingianins from *Endiandra kingiana*

Nur Amirah Saad,[a] Sharifah Mohammad,[b] Mohamad Hafizi Abu Bakar,[b] Mohammad Tasyriq Che Omar,[c] Marc Litaudon,[d] Khalijah Awang[e] and Mohamad Nurul Azmi[*,a]*

[a]*School of Chemical Sciences, Universiti Sains Malaysia, 11800 Minden, Pulau Pinang, Malaysia*

[b]*Bioprocess Technology Division, School of Industrial Technology, Universiti Sains Malaysia, 11800 Minden, Pulau Pinang, Malaysia*

[c]*School of Distance Education, Universiti Sains Malaysia, 11800 Minden, Pulau Pinang, Malaysia*

[d]*Institut de Chimie des Substances Naturelles, CNRS-ICSN UPR 01, Univ. Paris-Sud 11, Av. de la Terrasse, 91198 Gif-sur-Yvette, France*

[e]*Department of Chemistry, Faculty of Science, University of Malaya, 50603 Kuala Lumpur, Malaysia*

Diabetes has become a severe chronic disease worldwide with patients significantly increasing daily. Due to the side effects of insulin and oral hypoglycaemic agents employed in diabetes treatment, scientists are working hard to develop alternative approaches from natural plants that inhibit α-amylase and α-glucosidase. Consequently, by performing a phytochemical analysis on the bark of *Endiandra kingiana*, the present study isolated 11 cyclic polyketides. Analyses with one-dimensional and two-dimensional nuclear magnetic resonance (1D- and 2D-NMR), high-resolution electron ionization mass spectrometry (HRESIMS), and comparison with previous literature confirmed the compounds characteristics. Subsequently, the compounds were screened for *in vitro* α-amylase and α-glucosidase inhibiting activities. Compounds **9** and **2** exhibited potent inhibition towards α-amylase at 0.0008903 ± 0.5 and 0.02 ± 0.3 mg mL^{-1} of half-maximal inhibitory concentration (IC_{50}) values, respectively. In the α-glucosidase inhibition assay, compounds **10** and **5** demonstrated good inhibition with IC_{50} values of 0.11 ± 0.08 and 0.14 ± 0.05 mg mL^{-1}, respectively. The molecular docking examination demonstrated that the compounds adhered to the active sites on the C-terminal of the human pancreatic α-amylase (Protein Data Bank Identification (PDB ID): 2QV4, resolution: 1.97 Å) and maltase-glucoamylase (MGAM) (PDB ID: 3TOP, resolution: 2.88 Å), agreeing with α-amylase and α-glucosidase enzymes inhibitory reactions.

Keywords: *Endiandra kingiana*, endiandric acids, kingianins, α-amylase, α-glucosidase, molecular docking

Introduction

Diabetes mellitus (DM) is a metabolic affliction resulting from hyperglycemia due to inadequate pancreatic insulin production, defective insulin activity, or both.[1] A recurrent effect of uncontrolled diabetes is hyperglycemia that leads to dysfunction, failure, and acute organ damage, chiefly the eyes, kidneys, nerves, heart, and blood vessels.[2] Types I and II are the typical types of diabetes. Non-insulin-dependent diabetic patients are categorized as type II, the more frequent type of diabetes, constituting more than 90% of diabetic patients. Type II diabetes is often asymptomatic and undiagnosed at early stages.

In recent decades it was observed the steady rise of prevalence and patients of diabetes. Recently, diabetes has become a consequential chronic disease worldwide, with patients significantly increasing daily. The nineth edition of the Diabetes Atlas (2019) by the International Diabetes Federal (IDF) reported the most recent figures and projections on diabetes globally.[3] According to the report, approximately 463 million adults ages between

*e-mail: mnazmi@usm.my
Editor handled this article: José Walkimar M. Carneiro

20 and 79 have diabetes. Moreover, by 2045, the number is projected to reach 700 million. One out of five individuals above 65 years old is diabetic, while one in two, approximately 232 million, have undiagnosed diabetes.[3] Approximately 79% of diabetic adults reside in low- and middle-income nations. Meanwhile, 4.2 million deaths are unambiguously ascribed to diabetes in 2019. Approximately 1.5 million mortalities were directly due to diabetes in 2019, while in 2012, another 2.2 million deaths were attributed to elevated blood glucose levels.[4]

The World Health Organization (WHO) categorized diabetes as a treatable disease. Furthermore, its repercussions could be prevented or hindered with medication, a healthy diet, regular physical activity, and evaluations and medications for complications.[4] Common therapeutic approaches to treat diabetes is delaying carbohydrate absorption, lengthening carbohydrate digestion period in the gastrointestinal tract, and diminishing hyperglycemia, all of which could be achieved by impeding the actions of carbohydrates-hydrolyzing enzymes, including α-amylase and α-glucosidase.

There are three alpha-glucosidase inhibitors (AGIs) that are commonly used to inhibit the absorption of carbohydrates from the small intestine, which are acarbose, voglibose and miglitol.[5] Nonetheless, these drugs exhibited undesirable side effects, including flatulence, cramps, and hypoglycemia, typically linked to partial carbohydrate assimilation.[6] According to a review from Newman and Cragg,[7] approximately 29% of commercialized drugs are synthetic in origin and the rest are approved drugs from natural origin or natural products derived from natural products. Consequently, there is an urge to develop novel targeted antidiabetic drugs from natural plants.

Endiandra kingiana Gamble (*E. kingiana*) belongs to the Lauraceae or Laurel family. The Lauraceae family, also called Medang or Tejur, encompasses approximately 68 genera and 2980 species worldwide. The plant family grows mainly in the tropical regions, principally in Southeast Asia and tropical America.[8] Generally, the Lauraceae family comprises shrubs and trees that are evergreen and have no buttresses. Meanwhile, the genus *Endiandra* of the Laurel family contains over 125 plants in Southeast Asia, the Pacific region, and Australia. Over the past decades, *Endiandra* has been the subject of numerous investigations as it is widely utilized as traditional medicine other than *Beilschmiedia* of the same family.[9] Interestingly, the genus possesses a particular type of polyketide, which are endiandric acids and kingianins, extracted from the late-stage electrocyclisation of polyenes.[10]

Previously, some of the isolated compounds from *E. kingiana* were evaluated against antiapoptotic protein Bcl-xL, Mcl-1 and dengue virus type 2 NS2B/NS3 serine protease.[11-14]

A preliminary study demonstrated that *E. kingiana* extract displayed adequate inhibitory actions against α-amylase and α-glucosidase when its IC_{50} values were between 2.32 ± 0.0-8.93 ± 0.01 and 1.83 ± 0.03-716 ± 0.02 μg mL^{-1}, respectively.[15] Moreover, the primary compounds exhibited an interesting pattern in inhibiting α-glucosidase during the *in vitro* assays and molecular docking study with half-maximal inhibitory concentration (IC_{50}) values at 11.9 ± 2.0 μM (kingianin A) and 19.7 ± 1.5 μM (kingianin F), respectively.[16] Nevertheless, the present investigations intended to continue the interest in natural products isolated from Malaysian flora, especially *E. kingiana*. Additionally, the isolation, characterization, and hyperglycemic inhibitory activities of the isolated compounds were performed. The molecular docking section was also discussed to comprehend the interactivity between the isolated compounds and the active sites of the enzymes. Furthermore, the structure-activity relationships (SARs) predicted the physicochemical, biological, and environmental fates of the compounds based on their chemical structures.

Experimental

General experimental procedure

The majority of the chemicals employed in the present experiment were obtained commercially analytical grade and employed without additional purification unless stated. Column chromatography (CC) was conducted with silica gel 40-63 μm (Merck, Darmstadt, Germany). In thin layer chromatography (TLC), TLC silica gel 60 F_{254} aluminum plates (Merck, Darmstadt, Germany) were employed. The nuclear magnetic resonance (NMR) spectra were performed with Bruker Advance 500 (Bruker Bioscience, Billerica, Massachusetts, United States) at 500 and 125 MHz for ^{1}H and ^{13}C NMR spectrometer systems, respectively.

The data obtained were analyzed by employing the Top Spin 3.6.4 software package, while the spectra were denoted as tetramethylsilane (TMS) or residual solvent, deuterated chloroform ($CDCl_3$) at 7.26 ppm in ^{1}H NMR and 77.2 ppm in ^{13}C NMR. The ^{1}H NMR spectroscopic data identified chemical shift, relative integral, multiplicity (s represented singlets, d the doublets, and dd the doublet of doublets), and spin-spin coupling constants, *J*, in hertz (Hz). Additionally, mass spectrometry was performed utilizing high-resolution electron ionization mass spectrometry (HRESIMS) with Thermoquest TLM LCQ Deca ion-trap mass spectrometer (Thermoquest, Mississauga, Canada).

High-performance liquid chromatography (HPLC) (Waters®, Milford, Massachusetts, United States) was conducted in the fractions purification process. The Waters® X-Bridge C18 column (250 × 4.6 mm, 5.0 µm and 150 × 10.0 mm, 5.0 µm) was utilized during the analytical and semi-preparative HPLC analyses, performed with Waters auto purification system incorporated with a Waters 2767 sample manager, a column fluidics organizer, a Waters 2525 binary pump, a Waters 2996 ultraviolet-visible (UV-Vis) diode array detector (190-600 nm), and a PL-ELS 1000 ELSD Polymer Laboratory detector.

The isolated compounds were screened for their inhibiting actions against α-amylase and α-glucosidase by employing α-amylase (TCI, Saitama, Japan) from *Bacillus subtilis* and α-glucosidase (Sigma-Aldrich, Missouri, United States) from *Saccharomyces cerevisiae*. The screening was conducted with a microplate reader (Halo MPR-96, Dynamica, Victoria, Australia). Furthermore, molecular docking studies utilising AutoDock Vina[17] were implemented to explore the adhering interactivities of the active compounds. The structure-activity relationships were also observed to study the effects of chemical structures and potential inhibitory action on enzymes α-amylase and α-glucosidase.

The plant material

Barks of the *E. kingiana* Gamble plant were gathered in May 2006. The samples plants were identified at the Reserved Forest Sungai Temau, Kuala Lipis, Pahang, Malaysia. The *E. kingiana* was recognized by a botanist from the University of Malaya, Teo Leong Eng. A voucher specimen (KL 5243) was deposited at the Herbarium of the Department of Chemistry, Faculty of Science, University of Malaya, Kuala Lumpur, Malaysia.

Extraction, isolation, and characterization of chemical compounds

The desired chemical compounds were extracted, isolated, and characterized based on the methods outlined by Azmi *et al.*[12,13] The air-dried barks of *E. kingiana* (1.5 kg) were cut, ground, and extracted with 1.5 L of methanol (MeOH) three times using maceration process. The MeOH extract (118.3 g) was further partitioned with ethyl acetate (EtOAc) to obtain ethyl acetate crude extract. EtOAc-soluble extract was then proceeded to investigate its chemical constituents. First, the compound was examined via CC (SiO_2, 230-400 mesh) eluted with hexane/dichloromethane/MeOH by step gradient. Based on the TLC profile and ^{1}H NMR comparisons, the first fractionation afforded eight fractions, which henceforth were labelled EK_F1 to EK_F8.

The EK_F4 fraction was further fractionated with CC (SiO_2, 230-400 mesh, hexane/EtOAc step gradient), resulting in 20 sub-fractions, named EK_F4.1 to EK_F4.20. Subsequently, fractions EK_F4.3 to EK_F4.15 were further separated with HPLC to produce endiandric acid type A; kingianic acid B (**1**), kingianic acid C (**2**), kingianic acid E (**3**), endiandric acid M (**4**) while for endiandric acid type B, kingianic acid F (**5**) was obtained and for endiandric acid type B'; kingianic acid G (**6**) kingianic acid H (**7**) were isolated. Fractions EK_F5 to EK_F7 were subjected to an extensive purification process with CC and HPLC to yield kingianins series; kingianin K (**8**), kingianin L (**9**), kingianin M (**10**) and kingianin N (**11**).

The α-amylase inhibitory assay

The α-amylase inhibition assay employed the 3,5-dinitrosalicylic acid (DNSA) method as outlined by Abu Bakar *et al.*[15] All isolated compounds from the *E. kingiana* barks were weighed and dissolved with equivalent volumes of dimethyl sulfoxide (DMSO) and distilled water. A total of 250 µL of α-amylase solution was obtained by dissolving 0.05 g of the enzyme in 100 mL 20 mM phosphate buffer at pH 6.9. The solution was diluted with soluble starch at 1% weight *per* volume (m/v) before being added into tubes that each contained 250 µL of the isolated compounds and incubated for ten minutes at 25 °C. The reaction was ceased with the incorporation of 0.5 mL DNSA reagent (150 g sodium potassium tartrate, 8 g sodium hydroxide (NaOH), and 5 g 3,5-dinitrosalicylic acid powder dissolved in 500 mL distilled water). The resultant chemical was boiled in a water bath at 85-90 °C for five minutes. Subsequently, the mixture was cooled to surrounding temperature and diluted with 5 mL of distilled water.

The absorbance reading was assessed at 540 nm with an MPR-96 microplate reader (Halo, Dynamica, Australia). Acarbose solution was employed as the positive control sample, while the negative control was obtained by replacing the isolated compounds with buffer. Both control samples were subjected to the same reaction as the isolated compounds. The α-amylase inhibiting action was translated into the inhibition percentage and determined with equation 1. Subsequently, the percentage of α-amylase inhibition was plotted against the compound concentration, and the IC_{50} values were retrieved from the graph.

$$\text{Inhibition percentage}\,(\%) = \left(\frac{\text{Abs}_{\text{control}} - \text{Abs}_{\text{compound}}}{\text{Abs}_{\text{control}}}\right) \quad (1)$$

where $Abs_{control}$ is the absorbance value of the control solutions and $Abs_{compound}$ refers to the absorbance value of the isolated compounds.

The α-glucosidase inhibitory assay

The α-glucosidase inhibition assay was conducted as reported by Abu Bakar *et al.*[15] Initially, 3.827 g of α-glucosidase enzyme was dissolved in 100 mL of 20 mM phosphate buffer at pH 6.9 to acquire 1.0 U mL^{-1} α-glucosidase solution. The isolated compounds from *E. kingiana* were weighed and dissolved in equivalent volumes of DMSO and distilled water. Next, 100 µL of the α-glucosidase solution was poured into tubes that each contained 50 µL of the isolated compounds and were pre-incubated at 37 °C for ten minutes. Upon incubation, 50 µL of 4-nitrophenyl α-D-glucopyranoside (pNPG) (3.0 mM) was incorporated as a substrate. The resultant solution was further incubated for 20 min. Finally, the reaction was discontinued by introducing 2 mL of 0.1 M sodium carbonate (Na_2CO_3) into the mixture.

The absorbance reading was evaluated at 405 nm with an MPR-96 microplate reader (Halo, Dynamica, Australia). The positive and negative controls were subjected to the same reaction as the isolated compounds, utilizing the positive and negative solutions utilized in the α-amylase inhibition assay. The α-glucosidase inhibitory action was calculated with equation 2 and expressed as the inhibition percentage. A graph representing the percentage of α-glucosidase inhibition against compound concentration was plotted. The IC_{50} values were retrieved from the graph.

$$\text{Percentage of inhibition}\,(\%) = \left(\frac{\text{Abs}_{\text{control}} - \text{Abs}_{\text{compound}}}{\text{Abs}_{\text{control}}}\right) \quad (2)$$

where $Abs_{control}$ is the absorbance value of the control solutions and $Abs_{compound}$ corresponds to the absorbance value of the isolated compounds.

Molecular docking

The binding properties of the most potent compounds against α-amylase (Protein Data Bank (PDB) ID: 2QV4, resolution: 1.97 Å) and α-glucosidase (PDB ID: 3TOP, resolution: 2.88 Å) were determined through a docking study. Three-dimensional reference structures coordinates, including for the C-terminals of nitrite and acarbose complexed human pancreatic alpha-amylase (PDB ID: 2QV4, resolution: 1.97 Å)[18] and acarbose complexed maltase-glucoamylase (ctMGAM) (PDB ID: 3TOP, resolution: 2.88 Å),[19] were procured according to their ID from the Protein Data Bank (PDB) database to UCSF Chimera[20] version 1.15. Both crystal PDBs were subjected to the Dock Prep tool in Chimera to remove water molecules and unrelated heteroatom before docking. Subsequently, the receptor and inhibitor complexes were separated into discrete structures. Finally, the minimization process of singular structures through the steepest descent steps was conducted where the polar hydrogens and Gasteiger charges were added.[21] The diminished receptors and inhibitors were saved in PDB formats. The ChemDraw[22] was employed to create the compounds in cdx format before converting them to the PDB format.

A grid of 56, 72, and 57 along the X-, Y-, and Z-axes with 0.375 Å spacing was set to distinguish the binding sites in amylase. The grid centers along the X-, Y-, Z-axes were fixed at 18, 61, and 16 Å, respectively. Meanwhile, to recognize the adhering points in ctMGAM, the grid size was programmed to 86, 58, and 77, with 0.375 Å grid spacing on the X-, Y-, and Z-axes, respectively. The grid centers were placed at −47, 21, and 17 Å on the X-, Y-, and Z- axes, respectively. The viable bindings sites and binding energies[23] were determined by employing AutoDock Vina. For each of the tested compounds, the Dock score of the best postures docked into the target protein was computed as shown in Figure 1. The Biovia Discovery Studio Visualizer Client 2020[24] was used to analyze further the output obtained from AutoDock Vina.

Results and Discussion

Isolation and characterization

The current study examined the chemical compositions of the extract from the barks of *Endiandra kingiana* (KL5243) collected from Kuala Lipis Reserved Forest, Pahang, Malaysia. The isolation and purification processes were performed utilizing the standard and modern procedures, including CC and HPLC, respectively. The characterization and structural determination of compounds **1** to **11** were obtained with the assistance of spectroscopic procedures; 1D- and 2D-NMR combined with HRESIMS, and comparisons with published works (detailed in Supplementary Information (SI) section).[11-13]

Two categories of compounds were separated and characterized from the extract, the endiandric acid and the kingianin series. Four endiandric acids type A were isolated, which were kingianic acid B (**1**), kingianic acid C (**2**), kingianic acid E (**3**), endiandric acid M (**4**). Moreover, endiandric acid type B, kingianic acid F (**5**), and two endiandric acid type B', kingianic acid G (**6**) and kingianic acid H (**7**), were obtained. Additionally, four

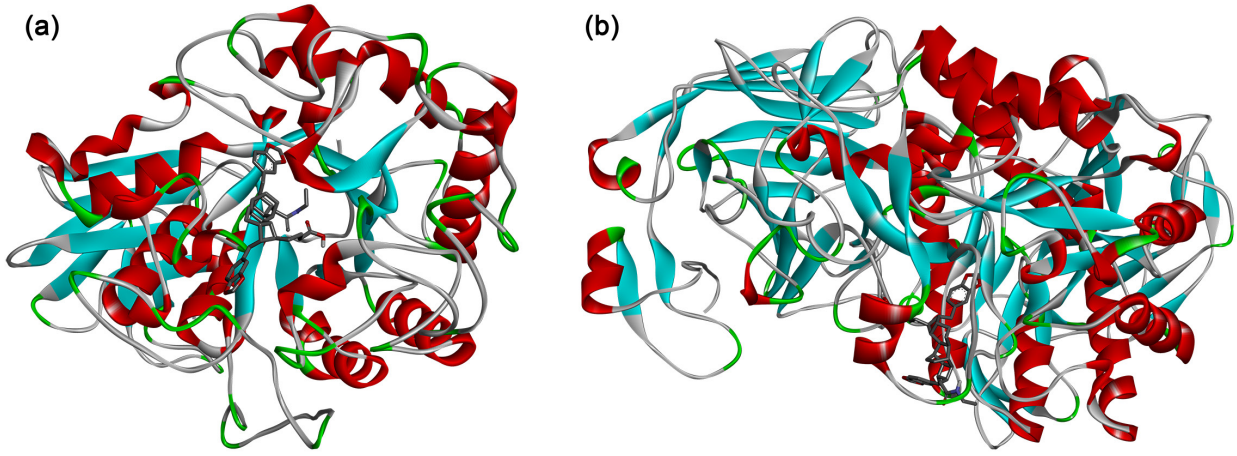

Figure 1. The best docked pose for compounds **9** with 2QV4 (a) and **10** with 3TOP (b) in Discovery Studio Visualiser.[24]

known pentacyclic kingianin series were isolated from the kingianin series, kingianin K (**8**), kingianin L (**9**), kingianin M (**10**) and kingianin N (**11**). The structures of the segregated molecules were displayed in Figure 2.

Endiandric acids are exclusively derived from the *Endiandra* and *Beilschmiedia* species and feature a unique tetracyclic carbon skeleton. Types A, B, and B' (Figure 2) were the three primary skeletal types of the cyclic polyketides, consisting of eight chiral centers and commonly isolated as racemic mixtures $[\alpha]_D = 0°$. Generally, a phenyl ring and a carboxylic acid chain substitute the backbone of the endiandric acids (types A, B, and B') that comprises two cyclohexanes, a cyclopentane, and a cyclobutane ring.

The kingianins were an optically inert white powder or amorphous solid with identical spectroscopic characteristics. The common compound property is the pentacyclic carbon skeleton (bicyclo[4.2.0] backbone). Nevertheless, the positions of the four substituents connected at the C-1, C-8, C-1', and C-8' distinguish the compounds from one another. Two substituents were methylenedioxyphenyl groups, while amide or acid groups made up the other two counterparts (Figure 3).

The α-amylase and α-glucosidase inhibitory assays

Published studies[25,26] suggested that the inhibition of α-amylase in the pancreas and the action of α-glucosidase in the intestine might combat diabetes by monitoring post-prandial glucose levels. In the present study, α-amylase and α-glucosidase suppressing actions were determined with acarbose as the positive control. The results are summarized in Table 1.

The isolated compounds exhibited diverse α-amylase and α-glucosidase restraining potentials. The IC_{50} values of α-amylase and α-glucosidase inhibition were within 0.0008903 ± 0.5 to 14.63 ± 1.5 and 0.11 ± 0.08 to 113.90 ± 1.16 mg mL^{-1}, respectively. Alternatively, the standard acarbose exhibited an IC_{50} value of 0.03 ± 0.01 mg mL^{-1} against α-amylase and 1.81 ± 0.1 mg mL^{-1} against α-glucosidase. Compounds **9** and **2** demonstrated the most potent inhibitors towards α-amylase with IC_{50} values of 0.0008903 ± 0.5 and 0.02 ± 0.3 mg mL^{-1}, respectively. Moreover, compound **9** demonstrated stronger inhibition activity against α-amylase at 100-fold inhibition compared to the standard acarbose.

Meanwhile, compounds **10** and **5** were the most potent inhibitors for α-glucosidase with IC_{50} values of 0.11 ± 0.08 and 0.14 ± 0.05 mg mL^{-1}, respectively. Furthermore, compound **10** exhibited approximately 10-fold inhibitory activity against α-glucosidase relative to acarbose. The observations indicated that compounds **9** and **10** were highly potent inhibitors of α-amylase and α-glucosidase, respectively, and potentially could be the lead molecules in regulating blood glucose levels of diabetic patients.

Based on Table 1, compounds **2**, **5**, **7**, **9**, and **10** demonstrated potential as dual inhibitors against both enzymes. The compounds might reduce starch hydrolysis and hence control diabetes. Moreover, due to the slow healing process, diabetes treatments often require a combination of both enzymes.[27] Consequently, the dual potentiality of the compounds might serve as the lead candidates for anti-diabetes drug compounds development.

Compounds **1** and **8** were mono inhibitors towards α-amylase with IC_{50} values of 14.63 ± 1.5 and 3.74 ± 1.3 mg mL^{-1}, respectively. Meanwhile, compounds **3**, **6**, and **11** were mono inhibitors against α-glucosidase with IC_{50} values of 0.69 ± 0.05, 0.26 ± 0.04, and 0.18 ± 0.03 mg mL^{-1}, respectively. The α-glucosidase mono inhibitors exhibited good inhibition compared to the positive control, acarbose, with an IC_{50} value of 1.81 ± 0.1 mg mL^{-1}.

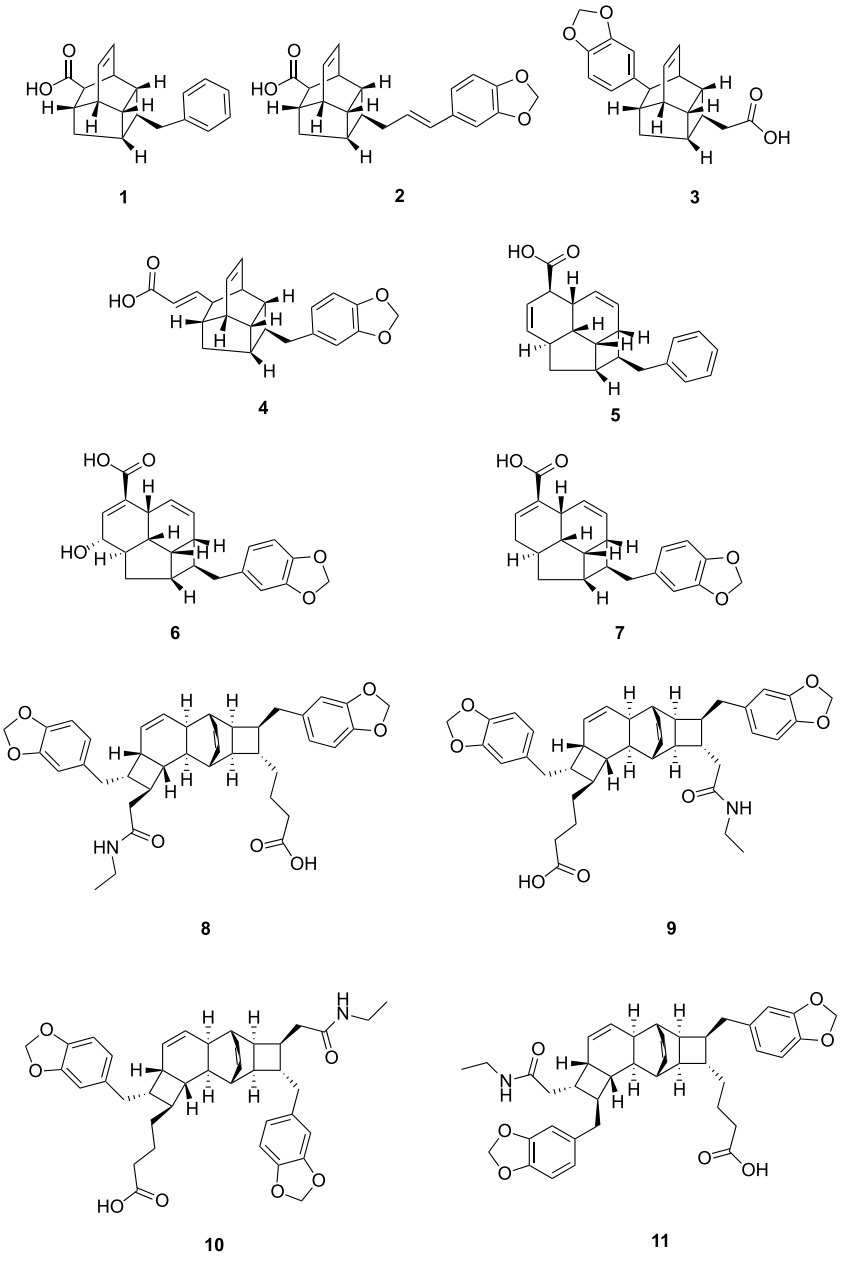

Figure 2. The structures of isolated cyclic polyketides, compounds **1** to **11**.

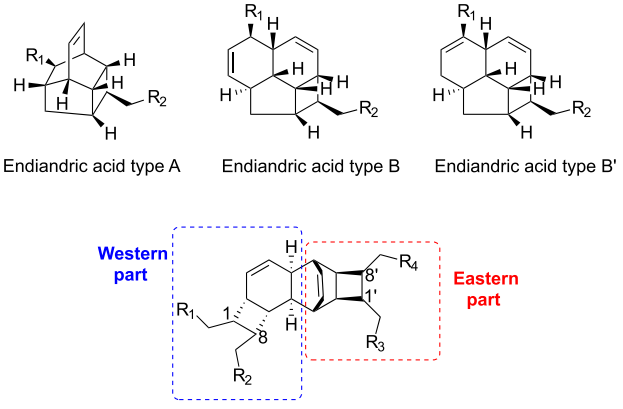

Figure 3. The endiandric acid and kingianin main skeletons.

Molecular docking

To further investigate the promising antidiabetic mechanisms of compounds **9**, **2**, **10**, and **5**, molecular docking studies were implemented on α-amylase and α-glucosidase enzymes by employing the AutoDock Vina program. The crystal structures of the C-terminal of human pancreatic α-amylase complexed with nitrite and acarbose (PDB ID: 2QV4, resolution: 1.97 Å)[28] and ctMGAM complexed with acarbose (PDB ID: 3TOP, resolution: 2.88 Å)[29] were utilized as the reference structures for the process. The docking results for the binding energies of potent compounds **9** and **2** were –9.7 and –9.9 kcal mol^{-1},

Table 1. The IC_{50} values for α-amylase and α-glucosidase inhibition for compounds **1** to **11**

Type of polyketides	Compound name	IC_{50} / (mg mL^{-1})	
		α-Amylase	α-Glucosidase
Endiandric acid type A (tetracyclic)	kingianic acid B (**1**)	3.74 ± 1.30	> 250
	kingianic acid C (**2**)	0.02 ± 0.30	0.28 ± 0.01
	kingianic acid E (**3**)	> 250	0.26 ± 0.04
	endiandric acid M (**4**)	NA	0.76 ± 0.06
Endiandric acid type B and B' (tetracyclic)	kingianic acid F (**5**)	7.43 ± 0.50	0.14 ± 0.05
	kingianic acid G (**6**)	> 250	0.18 ± 0.03
	kingianic acid H (**7**)	2.74 ± 0.20	0.22 ± 0.03
Kingianin (pentacyclic)	kingianin K (**8**)	14.63 ± 1.50	113.90 ± 1.16
	kingianin L (**9**)	0.0008903 ± 0.50	0.35 ± 0.05
	kingianin M (**10**)	0.77 ± 0.40	0.11 ± 0.08
	kingianin N (**11**)	> 250	0.69 ± 0.05
	acarbose	0.03 ± 0.01	1.81 ± 0.10

± standard deviation for n = 3 experiments. IC_{50}: half-maximal inhibitory concentration; NA: not available.

respectively, for α-amylase. The results were superior to the positive control, acarbose, at −8.4 kcal mol^{-1}. Meanwhile, potent compounds **5** and **10** exhibited −8.5 and 10.4 kcal mol^{-1}, respectively, for α-glucosidase that was also better than acarbose (see Table 2).

Table 2. The *in silico* binding energies of the potent compounds towards α-amylase and α-glucosidase (ctMGAM)

Enzyme	Compound name	Binding energy / (kcal mol^{-1})
α-Amylase	kingianin L (**9**)	−9.7
	kingianic acid C (**2**)	−9.9 ± 0.00
	acarbose	−8.4 ± 0.00
α-Glucosidase	kingianin M (**10**)	−10.4 ± 0.00
	kingianic acid F (**5**)	−8.5 ± 0.05
	acarbose	−8.1 ± 0.00

± standard deviation for n = 3 experiments.

The detailed interaction modes between most potent compounds and their excess in the active site of the human pancreatic α-amylase or C-terminal of the human maltase glucoamylase, ctMGAM (α-glucosidase), are listed in Table 3. Compound **9**, the most potent compound towards α-amylase, exhibited hydrogen bondings between the hydrogen atoms in hydroxyl and NH amide groups with Trp59 and Asp197, respectively. Seven hydrophobic interactions were formed between the cyclobutyl and phenyl rings of compound **9** and Trp59, His201, Ile235, and Leu162 (Figure 4a). Meanwhile, compound **2**, the second-most potent towards α-amylase, demonstrated hydrogen bonding between its hydroxyl group and oxygen in methylenedioxy with His305 and Lys200. Moreover, six hydrophobic interactions were observed between phenyl, cyclobutyl, and cyclopentyl rings with Lys200, Ile235, His201, Trp58, and Tyr62, while the His201 and Ile235 interacted with phenyl rings via π-π T-shaped and π-sigma (Figure 4b).

The most potent compound against α-glucosidase, compound **10**, demonstrated interactions between the hydrogen atoms of its hydroxyl groups with Asp1157, while

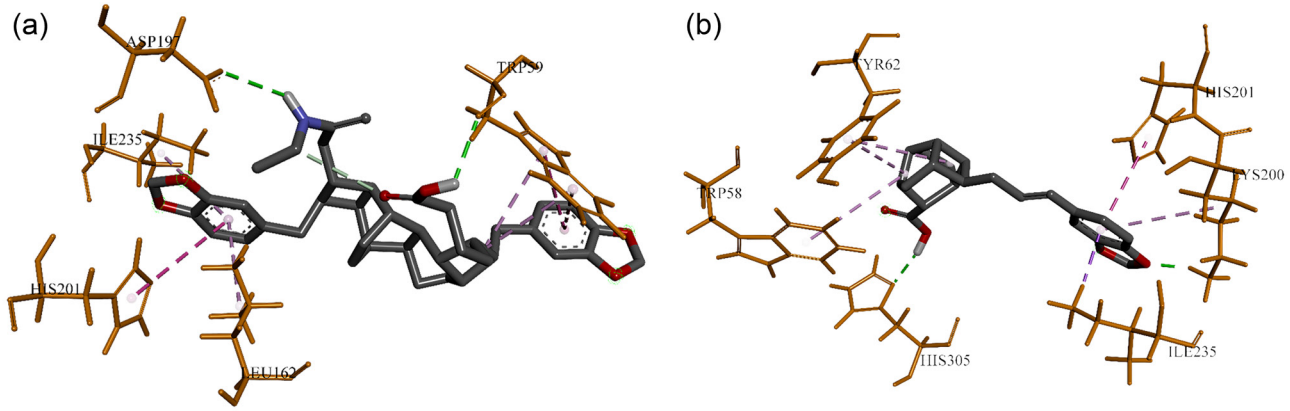

Figure 4. The three-dimensional binding modes of compounds **9** (a) and **2** (b) at the active sites of C-terminal of the human pancreatic α-amylase (PDB ID: 2QV4).

Table 3. The binding interactions between the active compounds and α-amylase or α-glucosidase (ctMGAM)

Protein	Compound	Free energy of binding / (kcal mol^{-1})	Protein residue	The interacting unit of the compound	Type of interaction
2QV4 (α-amylase)	kingianin L (**9**)	−9.7	Trp59	hydroxyl	H-bond
				cylobutyl	π-alkyl
				phenyl	π-π T-shaped/π-π stacked
			Asp197	NH amide	H- bond
			His201	phenyl	π-π T-shaped/π-π stacked
			Ile235	phenyl	π-alkyl
			Leu162	phenyl	π-alkyl
	kingianic acid C (**2**)	−9.9	His305	hydroxyl	H-bond
			Trp58	cyclopentyl	π-alkyl
			Tyr62	cyclopentyl	π-alkyl
				cyclobutyl	π-alkyl
			Lys200	methylenedioxyl	H-bond
				phenyl	π-alkyl
			Ile235	phenyl	π-sigma
			His201	phenyl	π-π T-shaped
	acarbose	−8.4	Gln63	hydroxyl	H-bond
			Thr163	hydroxyl	H-bond
			Leu165	carbonyl	alkyl
			Asp197	hydroxyl	H-bond
				carbonyl	H-bond
			Lys200	hydroxyl	unfavorable donor-donor
			His305	hydroxyl	H-bond
				hydroxyl	H-bond
3TOP (α-glucosidase)	kingianin M (**10**)	−10.4	Asp1157	hydroxyl	H-bond
			Gln1561	methylenedioxyl	H-bond
			Trp1355	cyclobutyl	π-alkyl
			Phe1560	cyclobutyl	π-alkyl
			Tyr1559	phenyl	π-π T-shaped
			Tyr1251	phenyl	π-π T-shaped
	kingianic acid F (**5**)	−8.5	Glu1629	hydroxyl	H-bond
			Trp1749	C=O	H-bond
				phenyl	π-π T-shaped
			Lys1625	cyclohexyl	alkyl
			Val1631	cyclohexyl	alkyl
			Pro1658	cyclohexyl	alkyl
				cyclobutyl	alkyl
				phenyl	π-alkyl
	acarbose	−8.1	Pro1359	hydroxyl	H-bond
				hydroxyl	H-bond
			Phe1358	hydroxyl	H-bond
			Gln1254	hydroxyl	H-bond
				hydroxyl	H-bond
			Arg1285	carbonyl	alkyl
				carbonyl	H-bond
			Ser1292	carbonyl	H-bond
			Met1283	carbonyl	H-bond carbon
			Asp1281	carbonyl	H-bond carbon
				carbonyl	H-bond carbon
			Gln1286	carbonyl	H-bond
				hydroxyl	H-bond

oxygen atoms from the methylenedioxyl groups interacted with Gln1561 through hydrogen bondings. Meanwhile, four hydrophobic interactions were formed between the phenyl and cyclobutyl rings of compound **10** with Phe1559, Tyr1251, Phe1560, and Trp1355, respectively, as displayed in Figure 5a. Compound **5**, which was the second most potent towards α-glucosidase, have hydrogen bonds formed between its hydroxyl and carbonyl groups with Glu1629 and Trp1749, respectively. Six hydrophobic interactions occurred between the phenyl, cyclohexyl, and cyclobutyl rings of the compound with Trp1749, Lys1625, Val1631, and Pro1658, as illustrated in Figure 5b.

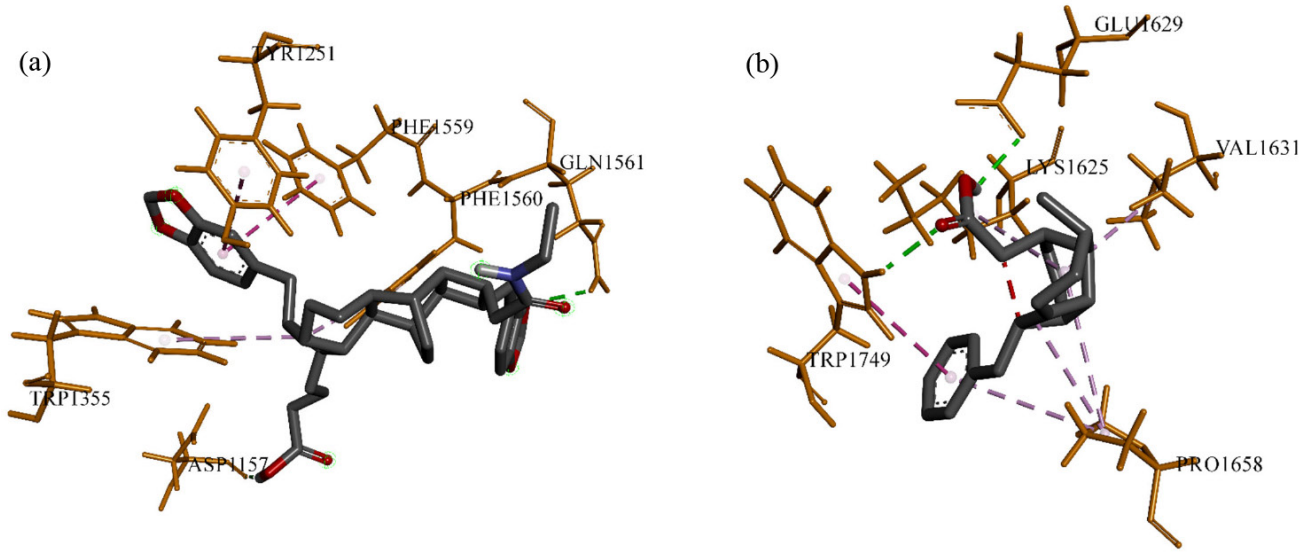

Figure 5. The three-dimensional binding modes of compounds (a) **10** and (b) **5** at the active sites of the human MGAM (PDB ID: 3TOP).

Alqahtani *et al.*[30] revealed that 3-oxolupenal and katononic acid produced a complex with α-glucosidase. The phenomenon was established with a static quenching mechanism via stabilization provided by a network of two to three hydrogen bonds and five to ten hydrophobic interactions. The molecular docking of compounds **9** and **2** and **10** and **5** in the C-terminal of the human pancreatic α-amylase and human MGAM, respectively, ranged between the number of networks of hydrogen bonds and hydrophobic interactions, supporting previous reports.[29-31] Moreover, the findings supported the *in vitro* α-amylase and α-glucosidase enzymes inhibitory actions of compounds **9** and **10**, respectively. The observations indicated that both compounds possessed the potential to be utilized in developing novel antidiabetic drugs.

The structure-activity relationship (SARs) studies

The SARs investigation corresponded to the impacts of chemical structures and the relationship between their potentials in inhibiting enzymes α-amylase and α-glucosidase. The pentacyclic compound with two methylenedioyphenyl, a butyric acid, and an *N*-ethylacetamide group was observed in kingianin series. Different substitutions at C-1, C-8, C-1', and C8' produced different compounds. The kingianin L (**9**), was favored for the efficacy of α-amylase inhibition, most frequently when the *N*-ethylacetamide was at C-1' and butanoic acid at C-8. As for the endiandric acid derivatives, α-amylase preferred kingianic acid C (**2**), which was endiandric acid type A. The compound with C-2' and C-3' double bond and methylenedioxyphenyl group were commonly favored. The α-glucosidase reacted more vigorously towards kingianin M (**10**) when the location of its butanoic acid at C-8 and *N*-ethylacetamide at C-8'. On the other hand, for the endiandric acid series, α-glucosidase favored endiandric acid type B, kingianic acid F (**5**), when the *cis* double bonds positions were at the C-4, C-5, C-8, and C-9 with a phenyl group. In conclusion, α-amylase and α-glucosidase favored the kingianin series to the endiandric acid series. The structure requirements of kingianin series for α-amylase and α-glucosidase inhibition activities were summaries as follows (Figure 6).

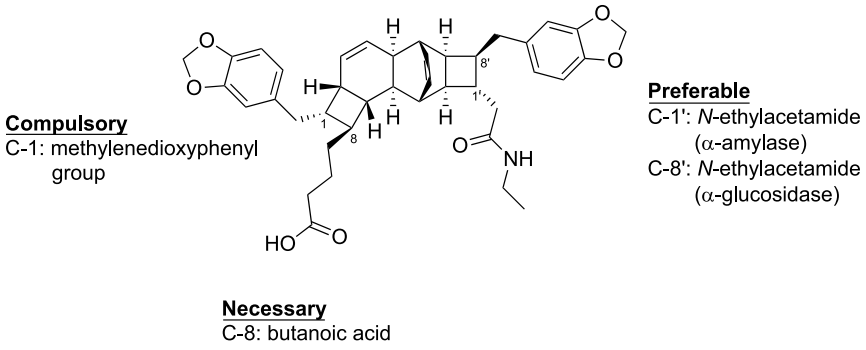

Figure 6. Structure-activity relationships (SARs) studies of kingianin series.

Conclusions

In the present study, 11 compounds were isolated from the bark of *Endiandra kingiana* and exhibited varying degrees of inhibitory actions against α-amylase and α-glucosidase. Compound **9** demonstrated potent α-amylase inhibition activity with the IC_{50} value of 0.0008903 ± 0.5 mg mL^{-1}, 100-fold superior than acarbose at IC_{50} = 0.03 ± 0.01 mg mL^{-1}. Meanwhile, compound **10** exhibited adequate inhibition towards α-glucosidase with an IC_{50} value of 0.11 ± 0.08 mg mL^{-1}, which were 10-fold better than acarbose (IC_{50} = 1.81 ± 0.1 mg mL^{-1}). Moreover, the molecular docking findings agreed with the observations for the *in vitro* inhibition activities of α-amylase and α-glucosidase enzymes. Consequently, the substances might be considered the lead candidates for drug development for treating diabetics.

Supplementary Information

Supplementary information (^{1}H NMR, ^{13}C NMR, HRMS spectra and 2D binding modes for some important compounds) is available free of charge at http://jbcs.sbq.org.br as PDF file.

Acknowledgments

This research was financially funded through Universiti Sains Malaysia Research Grant RUI (1001. PKIMIA.8012310). This research was conducted within the frame of the collaboration between USM-CNRS (LoI) and auspices of CNRS-UM; Associated International Laboratory (LIA) under FM-NatProLab.

Author Contributions

Nur Amirah Saad was responsible for methodology, formal analysis, investigation, data curation, writing-original draft preparation, visualization; Sharifah Mohammad for methodology, formal analysis, investigation, data curation; Mohamad Hafizi Abu Bakar for methodology, validation, formal analysis, investigation, resources, writing-review and editing, supervisor; Mohammad Tasyriq Che Omar for methodology, software, validation, formal analysis, investigation, resources, writing-review and editing, supervisor; Marc Litaudon for investigation, writing-review and editing; Khalijah Awang for validation, writing-review and editing; Mohamad Nurul Azmi for conceptualization, methodology, validation, formal analysis, writing-original draft preparation, writing-review and editing, visualization, supervision, project administration, funding acquisition.

References

1. Abu Bakar, M. H.; Sarmidi, M. R.; Cheng, K. K.; Ali Khan, A.; Suan, C. L.; Zaman Huri, H.; Yaakob, H.; *Mol. BioSyst.* **2015**, *11*, 1742. [Crossref]
2. *Diabetes Care* **2002**, *25*, s21. [Crossref]
3. International Diabetes Federation (IDF); About Diabetes, https://idf.org/aboutdiabetes/what-is-diabetes/facts-figures.html, accessed in April 2022.
4. World Health Organization (WHO); Diabetes; https://www.who.int/news-room/fact-sheets/detail/diabetes, accessed in April 2022.
5. Derosa, G.; Maffioli, P.; *Arch. Med. Sci.* **2012**, *8*, 899. [Crossref]
6. Gulati, V.; Gulati, P.; Harding, I. H.; Palombo, E. A.; *BMC Complementary Altern. Med.* **2015**, *15*, 435. [Crossref]
7. Newman, D. J.; Cragg, G. M.; *J. Nat. Prod.* **2012**, *75*, 311. [Crossref]
8. Lauraceae -The Plant List, http://www.theplantlist.org/browse/A/Lauraceae/, accessed in April 2022.
9. Lenta, B.; Chouna, J.; Nkeng-Efouet, P.; Sewald, N.; *Biomolecules* **2015**, *5*, 910. [Crossref]
10. Taib, M. N. A. M.; Six, Y.; Litaudon, M.; Awang, K.; *Isolation and Identification of Cyclic Polyketides from Endiandra kingiana Gamble (Lauraceae), as Bcl-Xl/Bak and Mcl-1/Bid Dual Inhibitors, and Approaches Toward the Synthesis of Kingianins*; Ecole Doctorale Polytechnique: France, 2015. [Link] accessed in April 2022
11. Leverrier, A.; Awang, K.; Guéritte, F.; Litaudon, M.; *Phytochemistry* **2011**, *72*, 1443. [Crossref]
12. Azmi, M. N.; Saad, N. A.; Bakar, M. H. A.; Omar, M. T. C.; Aziz, A. N.; Wahab, H. A.; Al., E.; *Rec. Nat. Prod.* **2021**, 227. [Crossref]
13. Azmi, M. N.; Péresse, T.; Remeur, C.; Chan, G.; Roussi, F.; Litaudon, M.; Awang, K.; *Fitoterapia* **2016**, *109*, 190. [Crossref]
14. Sulaiman, S. N.; Hariono, M.; Salleh, H. M.; Chong, S. L.; Yee, L. S.; Zahari, A.; Wahab, H. A.; Derbré, S.; Awang, K.; *Nat Prod Commun*. **2019**, *14*, 1934578X19861014. [Crossref]
15. Abu Bakar, M. H.; Lee, P. Y.; Azmi, M. N.; Syifa'Lotfiamir, N.; Mohamad, M. S. F.; Shahril, N. S. N.; Shariff, K. A.; Ya'akob, H.; Awang, K.; Litaudon, M.; *Biocatal. Agric. Biotechnol.* **2020**, *25*, 101594. [Crossref]
16. Azmi, M. N.; Gény, C.; Leverrier, A.; Litaudon, M.; Dumontet, V.; Birlirakis, N.; Guéritte, F.; Leong, K. H.; Halim, S. N. A.; Mohamad, K.; Awang, K.; *Molecules* **2014**, *19*, 1732. [Crossref]
17. *AutoDock Vina*, version 1.1.2; The Scripps Research Institute, USA, 1989.
18. RCSB PDB-2QV4: Human Pancreatic Alpha-Amylase Complexed with Nitrite and Acarbose, https://www.rcsb.org/structure/2QV4, accessed in April 2022.

19. RCSB PDB-3TOP: Crystral Structure of the C-terminal Subunit of Human Maltase-Glucoamylase in Complex with Acarbose, https://www.rcsb.org/structure/3TOP, accessed in April 2022.
20. Resource for Biocomputing, Visualization, and Informatics (RBVI); *UCSF Chimera*, version 1.15; University of California, San Francisco, USA, 2020.
21. Kim, K.-T.; Rioux, L.-E.; Turgeon, S. L.; *Phytochemistry* **2014**, *98*, 27. [Crossref]
22. *ChemDraw*, version 20.0; Harvard University, Cambridge, USA, 1986.
23. Coussens, N. P.; Sittampalam, G. S.; Guha, R.; Brimacombe, K.; Grossman, A.; Chung, T. D. Y.; Weidner, J. R.; Riss, T.; Trask, O. J.; Auld, D.; Dahlin, J. L.; Devanaryan, V.; Foley, T. L.; McGee, J.; Kahl, S. D.; Kales, S. C.; Arkin, M.; Baell, J.; Bejcek, B.; Gal-Edd, N.; Glicksman, M.; Haas, J. V.; Iversen, P. W.; Hoeppner, M.; Lathrop, S.; Sayers, E.; Liu, H.; Trawick, B.; McVey, J.; Lemmon, V. P.; Li, Z.; McManus, O.; Minor, L.; Napper, A.; Wildey, M. J.; Pacifici, R.; Chin, W. W.; Xia, M.; Xu, X.; Lal-Nag, M.; Hall, M. D.; Michael, S.; Inglese, J.; Simeonov, A.; Austin, C. P.; *Clin. Transl. Sci.* **2018**, *11*, 461. [Crossref]
24. Dassault Systèmes; *Biovia Discovery Studio Visualizer Client 2020*, version 3.5; Discovery Studio Modeling Environment, San Diego, USA, 2017.
25. Sudha, P.; Zinjarde, S. S.; Bhargava, S. Y.; Kumar, A. R.; *BMC Complementary Altern. Med.* **2011**, *11*, 5. [Crossref]
26. Rosa, M. M.; Dias, T. In *Handbook of Clinical Neurology*, vol. 120; Elsevier: New York, 2014.
27. Poovitha, S.; Parani, M.; *BMC Complementary Altern. Med.* **2016**, *16*, 185. [Crossref]
28. Maurus, R.; Begum, A.; Williams, L. K.; Fredriksen, J. R.; Zhang, R.; Withers, S. G.; Brayer, G. D.; *Biochemistry* **2008**, *47*, 3332. [Crossref]
29. Ren, L.; Qin, X.; Cao, X.; Wang, L.; Bai, F.; Bai, G.; Shen, Y.; *Protein Cell* **2011**, *2*, 827. [Crossref]
30. Alqahtani, A. S.; Hidayathulla, S.; Rehman, M. T.; ElGamal, A. A.; Al-Massarani, S.; Razmovski-Naumovski, V.; Alqahtani, M. S.; El Dib, R. A.; AlAjmi, M. F.; *Biomolecules* **2019**, *10*, 61. [Crossref]
31. Sim, L.; Quezada-Calvillo, R.; Sterchi, E. E.; Nichols, B. L.; Rose, D. R.; *J. Mol. Biol.* **2008**, *375*, 782. [Crossref]

Submitted: February 24, 2022
Published online: Abril 25, 2022